Inverse Obstacle Scattering Using Reduced Data

Rainer Kress† and William Rundell‡

Abstract: The classical result of Schiffer in acoustic scattering is that a knowledge of the far field pattern for all observation directions and all incident directions at a fixed wave number k uniquely determines the sound-soft scattering obstacle D. This is widely believed to be far greater information than is required for uniqueness and more recent results have been obtained that considerably weaken the amount of data needed provided certain restrictions are placed on the scatterer. Most of this work has concentrated on reducing the number of incident waves required for a unique determination. This paper will take another approach and seeks to determine sufficient information to recover the obstacle from measurements of the far field at isolated points. Our approach will be constructive and some numerical reconstructions will be presented.

AMS (MOS) subject classification primary 81U40, 65R30; secondary 35J05.

1. Introduction

The standard problem in inverse obstacle scattering for time-harmonic acoustic waves is to determine the shape of an obstacle D from a measurement of the far field pattern u_∞ of the scattered wave u^s for a set of incident plane waves $u^i(x) = e^{ik\,d\cdot x}$ with direction of propagation d. The scattering of time-harmonic acoustic or electromagnetic waves at a cylindrical obstacle is modeled by the exterior boundary value problem for the Helmholtz equation

$$\triangle u + k^2 u = 0 \quad \text{in } \mathbb{R}^2 \setminus \bar{D} \tag{1}$$

with positive wave number k and Dirichlet boundary condition

$$u = 0 \quad \text{on } \partial D. \tag{2}$$

The Dirichlet conditions (2) corresponds to a sound-soft obstacle in acoustics or a perfectly conducting obstacle in electromagnetics. The total wave $u = u^i + u^s$ is decomposed into the given incident wave u^i and the unknown scattered wave u^s which is required to satisfy the Sommerfeld radiation condition

$$\frac{\partial u^s}{\partial r} - iku^s = o\left(\frac{1}{\sqrt{r}}\right), \quad r = |x| \to \infty, \tag{3}$$

uniformly in all directions $\hat{x} = x/|x|$. The Sommerfeld radiation condition is equivalent to the asymptotic behaviour

$$u^s(x) = \frac{e^{ik\,x}}{\sqrt{|x|}}\left(u_\infty(\hat{x};d) + O\left(\frac{1}{|x|}\right)\right), \quad |x| \to \infty, \tag{4}$$

†Institut für Numerische und Angewandte Mathematik, Universität Göttingen, 37083 Göttingen, Germany

‡Department of Mathematics, Texas A&M University, College Station, Texas 77843-3368.
This author acknowledges thanks for partial support from the National Science Foundation.

where the amplitude factor u_∞ is known as far field pattern of the scattered wave. It is defined on the unit circle in $\mathbb{R}^2$, a set which we will denote by Ω, and it depends both on the observation direction $\hat{x}$ and the incident direction d. The *inverse problem* now consists in the reconstruction of the scatterer D from a knowledge of the far field pattern u_∞.

The classical uniqueness theorem for this problem is due to Schiffer [LP] and states that a knowledge of the far field pattern $u(\hat{x}; d)$ for all observation directions $\hat{x} \in \Omega$ and all incident directions $d \in \Omega$ at a fixed wave number k uniquely determines the sound-soft or perfectly conducting scattering obstacle D.

In the more than three decades since Schiffer proved his theorem there have been numerous attempts to reduce the amount of data required. There is widespread belief based on some analysis and many numerical experiments that a measurement of the far field pattern for a single incident direction suffices to determine the scattering object, at least in the sound-soft or perfectly conducting case.

Indeed, based on Schiffer's ideas, Colton and Sleeman [CS] were able to show that D is uniquely determined by the far field pattern for a finite number of incident plane waves provided a priori information on the size of the obstacle is available. In particular, given the a priori information that the scatterer is contained in a disk of radius R then it is uniquely determined by the far field pattern for one incident plane wave provided the wave number satisfies $kR < \zeta_0$ where ζ_0 denotes the smallest positive zero of the Bessel function J_0 of order zero.

There are two recent uniqueness results of some interest: Potthast [Po] has proven that two obstacles which lie within a distance of ϵ of each other and share the same far field patterns for $N(\epsilon)$ incident waves must be identical. Using a different method Liu and Nachman [LN] have shown that there is at most a finite number of bounded, Lipschitz obstacles that can share the same far field pattern arising from a single incident wave. Further, a convex polyhedron is uniquely determined from this data.

Taking another approach, the present authors were able to obtain a local uniqueness result for obstacles sufficiently close to a circle. This allowed the consideration of an obstacles whose boundary lay in some finite dimensional set S and which could be recovered from the far field pattern at a discrete set of values for a single incident wave [KR1].

While the proof of Schiffer's theorem does not itself lead to a constructive approach, many numerical schemes have been developed to reconstruct the obstacle from these data measurements. Most of these have relied on optimisation techniques, see [CK]. However, the result of [KR1] led naturally to a constructive method and in particular the authors were able to characterise the degree of ill-posedness of the problem as a function of the wave number k and the dimension of the underlying basis set S for the class of admissible obstacles. In fact, an even stronger result is likely; in [KR2] the authors presented numerical evidence that the shape (but not the location) of the obstacle can be successfully reconstructed from only the amplitude of the far field pattern.

This paper will investigate the possibilities of obtaining local uniqueness results from considerably less data data than indicated by the Schiffer result. We will consider two such problems. The first seeks to recover the obstacle from knowledge of the far field pattern $u_\infty(\hat{x}; d)$ at a single observation direction $\hat{x} = Qd$ for all incident directions $d \in \Omega$ where Q is a fixed rotation matrix. In particular, this includes the case of backscattering. The second considers the case of a set of incident waves all from a

fixed direction, but with frequencies varying over an interval of k values. Data consists of values of the far field pattern at a finite number of directions for each value of k. We will show that unique recovery is possible for the first problem provided the wave number is sufficiently small. For the second it will be shown that two measurement directions, judiciously chosen, will also suffice.

As in [KR1], our approach will be through an explicit representation for the Fréchet derivative of the map F from the obstacle boundary ∂D to the far field pattern u_∞ using a domain derivative approach. This technique goes back to the very foundations of the subject, but the formulation we shall use is due to Kirsch [Kr]. From this we will be able to show local invertibility and the derivative so obtained will be used in an iterative method to obtain effective numerical reconstructions.

For the Schrödinger equation with backscattered data Eskin and Ralston [ER1], [ER2] have shown that the backscattering map is a local analytic homeomorphism in a small neighbourhood of a certain set of potentials. Recently, Stefanov and Uhlmann [SU] have given a uniqueness result for inverse potential scattering with backscattering for all incident directions and all frequencies. To our knowledge nothing is known on uniqueness for the inverse obstacle scattering problem for the Helmholtz equation with backscattering data.

2. Computation of the Fréchet Derivative

In this section, we will collect some known results for the derivative of the mapping F from an obstacle ∂D to the far field pattern u_∞. We will develop a general representation which will then be used to obtain properties of the derivatives for the maps under consideration. We assume that the boundary ∂D is starlike with respect to the origin, i.e., ∂D can be represented in the parametric form

$$\partial D = \{(r(t)\cos t, r(t)\sin t) : t \in [0, 2\pi]\}$$

with a positive, twice continuously differentiable, 2π periodic function $r : [0, 2\pi] \to \mathbb{R}$ representing the radial distance from the origin. The solution to the direct scattering problem (1) – (3) with a fixed incident wave u^i defines an operator

$$F : C_+^2[0, 2\pi] \to L^2(\Omega) \tag{5}$$

which maps the radial function r into the far field pattern u_∞ of the scattered wave u^s for the obstacle described by (5). Here, $C_+^2[0, 2\pi]$ is the cone of positive functions in $C^2[0, 2\pi]$. We can in fact reduce this regularity assumption but, for our present purposes, the effort would not be repaid. Given a (measured) far field pattern u_∞, in terms of the operator F, the inverse problem now is equivalent to solving the equation

$$F(q) = u_\infty \tag{6}$$

for the radial function $q(\theta)$ representing the boundary curve ∂D.

Instead of the usual Fourier representation of a real valued periodic function

$$q(t) = \sum_{m=0}^{\infty} \alpha_m \cos mt + \sum_{m=1}^{\infty} \beta_m \sin mt \tag{7}$$

we choose the complex form of the boundary representation

$$q(t) = \sum_{m=-N}^{N} a_m e^{i\,m\,t} \tag{8}$$

where N can be infinite and where

$$a_m = \frac{1}{2}\,(\alpha_m - i\beta_m), \quad a_{-m} = \frac{1}{2}\,(\alpha_m + i\beta_m).$$

In the sequel, we will express the directions $d = (\cos\theta_0, \sin\theta_0)$, $\hat{x} = (\cos\theta, \sin\theta)$ in terms of the incident angle θ_0 and the observation angle θ. Now from [KR1], the value of the Fréchet derivative of the mapping F in a direction q about the circle $r = 1$ is

$$(F'q)(\theta) = e^{-\frac{\pi i}{4}}\sqrt{\frac{2}{\pi k}}\sum_{n=-\infty}^{\infty}\frac{c_n}{i^n\,H_n^{(1)}(k)}\,e^{in\theta} \tag{9}$$

where

$$c_n := \frac{2i}{\pi}\sum_{m=-\infty}^{\infty} a_m\,\frac{i^{n-m}e^{i(m-n)\theta_0}}{H_{n-m}^{(1)}(k)} \tag{10}$$

and we note that the series (9) converges uniformly.

We are interested in the situation where the far field is measured with a fixed angle γ between the the incident angle θ_0 and the observation angle θ. Thus we will write $\theta = \theta_0 + \gamma$. Our formulae will be simpler if we choose the origin of our coordinate system at the point $t = \gamma/2$ and so instead of (8) we use

$$q(t) = \sum_{m=-\infty}^{\infty} a_m e^{i\,m(t-\gamma/2)} \tag{11}$$

Then from (9), (10) and (11) it can be shown that the derivative takes the form

$$(F'q)(\theta_0+\gamma, k) = \sqrt{\frac{8}{\pi^2 k}}\,e^{i\frac{\pi}{4}}\sum_{m=-\infty}^{\infty} a_m\,B_m(\gamma,k)\,e^{im\theta_0} \tag{12}$$

where

$$B_m(\gamma,k) := \frac{1}{i^m}\sum_{n=-\infty}^{\infty}\frac{1}{H_n^{(1)}(k)H_{n-m}^{(1)}(k)}\,e^{i(n-\frac{m}{2})\gamma}. \tag{13}$$

We can write the above as

$$B_m(\gamma,k) = \begin{cases} (-1)^{\frac{m}{2}}\Big[\dfrac{1}{H_{\frac{m}{2}}(k)H_{-\frac{m}{2}}(k)} \;+\; 2\displaystyle\sum_{n=\frac{m}{2}+1}^{\infty}\frac{\cos(n-\frac{m}{2})\gamma}{H_n(k)H_{n-m}(k)}\Big] & \text{if } m \text{ is even,} \\ 2(-1)^{\frac{m-1}{2}}\displaystyle\sum_{n=\frac{m+1}{2}}^{\infty}\frac{\sin(n-\frac{m}{2})\gamma}{H_n(k)H_{n-m}(k)} & \text{if } m \text{ is odd,} \end{cases}$$

which indicates the importance that the parity of m plays. The sequence B_m will play a prominent role in the analysis to follow and we collect some of the important properties below. We shall drop the suffix on the Hankel functions, it being understood they are of the first kind.

Lemma 1. *For all $\gamma \in (0, 2\pi)$ and $k > 0$ we have that $B_{-m}(\gamma,k) = (-1)^m B_m(\gamma,k)$ for all m and $B_m(0,k) = 0$ for m odd.*

Proof: We use the Bessel function identities $H_{-n} = (-1)^n H_n$ to obtain

$$\begin{aligned} B_{-m}(\gamma,k) &= \frac{1}{i^{-m}}\sum_{n=-\infty}^{\infty}\frac{e^{i(n+\frac{m}{2})\gamma}}{H_n(k)H_{n+m}(k)} \\ &= \frac{(-1)^m}{i^m}\sum_{n'=-\infty}^{\infty}\frac{e^{i(n'-\frac{m}{2})\gamma}}{H_{n'-m}(k)H_{n'}(k)} = (-1)^m B_m(\gamma,k) \end{aligned}$$

from which the first part follows directly. For the second part we note that

$$B_m(0,k) = \sum_{n'=-\infty}^{\infty} \frac{i^{-m}}{H_{n'+m}(k)H_{n'}(k)} = \sum_{n'=-\infty}^{\infty} \frac{i^{-m}}{H_{m-n'}(k)H_{-n'}(k)}$$
$$= \sum_{n'=-\infty}^{\infty} \frac{(-1)^m i^{-m}}{H_{n-m}(k)H_n(k)} = (-1)^m B_m(0,k).$$

Lemma 2. *For k sufficiently small and all $\gamma \in [0, 2\pi]$ we have that*

$$B_0(\gamma,k) = \frac{\pi^2}{4\ln^2\frac{k}{2}} + O(k^2), \quad B_m(\gamma,k) = g_m(\gamma)\,k^m + h_m(\gamma)\frac{k^m}{\ln\frac{k}{2}} + O(k^{m+2}), \quad m > 0,$$

uniformly with respect to m where

$$g_0(\gamma) = g_1(\gamma) = 0, \qquad g_m(\gamma) = -\frac{\pi^2}{4\,(m-2)!}\,\sin^{m-2}\frac{\gamma}{2}, \quad m \geq 2,$$

and

$$h_m(\gamma) = \begin{cases} \dfrac{\pi^2}{2^{m-1}(m-1)!}\,(-1)^{\frac{m}{2}}\,\cos\dfrac{m\gamma}{2} & \text{if } m \text{ is even,} \\ \dfrac{\pi^2}{2^{m-1}(m-1)!}\,(-1)^{\frac{m-1}{2}}\,\sin\dfrac{m\gamma}{2} & \text{if } m \text{ is odd.} \end{cases}$$

Proof: We use the asymptotic expansions

$$Y_0(k) = \frac{2}{\pi}\ln\frac{k}{2} + O(k^2\ln k), \qquad Y_n(k) = -\frac{1}{\pi}\frac{2^n}{k^n}\,(n-1)!\,(1+O(k^2)), \quad n \geq 1,$$

for small k which are uniformly valid with respect to n. Note that there are two terms in the series representing B_m containing a Hankel function of order zero and these give the contribution

$$\frac{1}{i^m}\Big[\frac{e^{i(-\frac{m}{2})\gamma}}{H_0^{(1)}(k)H_{-m}^{(1)}(k)} + \frac{e^{i(m-\frac{m}{2})\gamma}}{H_m^{(1)}(k)H_0^{(1)}(k)}\Big]$$
$$= -\frac{\pi^2}{2^{m-1}(m-1)!}\frac{1}{i^m}\big[e^{i(\frac{m}{2})} + (-1)^m e^{-i(\frac{m}{2})}\big]h_m k^m\,\frac{1}{\ln(k/2)}$$

where h_m is defined above. If $m = 0$ then it is easily seen that the lowest order term in k not containing $H_0(k)$ must come from the contribution of $1/H_n(k)H_n(k)$ with $n = \pm 1$ and these terms are of order k^2. The lowest order term arises from the product of the two Hankel terms of order zero and has value $\pi^2/4\ln^2(k/2)$. If $m = 1$ then the lowest terms not including $H_0(k)$ are of order k^3. This implies that $g_m = 0$ for $m = 0, 1$. For $m \geq 2$, the terms of order k^m are contributed by the combinations

$$\frac{1}{i^m}\sum_{n=1}^{m-1}\frac{e^{i(n-\frac{m}{2})\gamma}}{H_n^{(1)}(k)H_{n-m}^{(1)}(k)} = g_m(\gamma)k^m + O(k^{m+2})$$

where, by the binomial formula,

$$g_m(\gamma) = -\frac{\pi^2(-1)^m}{2^m i^m}\sum_{n=1}^{m-1}\frac{(-1)^n\,e^{i(n-\frac{m}{2})\gamma}}{(n-1)!\,(m-n-1)!} = -\frac{\pi^2}{4\,(m-2)!}\Big(\frac{e^{i\gamma/2}-e^{-i\gamma/2}}{2i}\Big)^{m-2}$$

as claimed in the statement of the lemma.

Corollary. *For k sufficiently small and any $\gamma \neq 0$ we have for all m that $B_m(\gamma,k) \neq 0$.*

3. Uniqueness Results

For the single frequency, multiple incident direction case we let θ_i, $i = 1, 2, \ldots$ be a set of incident directions and denote by $u_{\infty,i}$ the (complex-valued) farfield pattern measured at the single observation angle $\theta_i + \gamma$ that arises from the wave with incident direction θ_i and with fixed frequency k. Let F_{inc} be the map that takes an obstacle ∂D onto the set of values $\{u_{\infty,i}\}_{i=1}^{\infty}$. The offset γ between the incident and measured directions is fixed; the value $\gamma = \pi$ corresponds to the backscattering case and $\gamma = 0$ to the forward scattering situation.

For the case when the obstacle D is the unit disc we can use (12) to obtain the representation

$$F'_{\text{inc}}.q = \sqrt{\frac{8}{\pi^2 k}}\, e^{i\frac{\pi}{4}} \Bigg[\sum_{\substack{m=0 \\ m=\text{even}}}^{\infty} \{\alpha_m \cos m\theta_0^j - \beta_m \sin m\theta_0^j\} B_m(\gamma, k) + i \sum_{\substack{m=1 \\ m=\text{odd}}}^{\infty} \{\alpha_m \sin m\theta_0^j + \beta_m \cos m\theta_0^j\} B_m(\gamma, k). \Bigg] \tag{14}$$

From (14) it is clear that $F'_{\text{inc}} q = 0$ for all directions θ_0^i, where $\{\theta_i\}$ has a point of accumulation on the unit circle, implies that the sequences $\{B_m(\gamma, k)\, \alpha_m\}$ and $\{B_m(\gamma, k)\, \beta_m\}$ are identically zero. Now if k is sufficiently small, and $\gamma \neq 0$, it follows from the corollary to Lemma 2 that B_m has no zeroes, and hence the pair of sequences $\{\alpha_m\}$ and $\{\beta_m\}$ must be zero, showing that $q = 0$. Thus under these conditions on k and γ the map F'_{inc} is one to one.

We note that if γ is zero, the forward scattering case, then from Lemma 1 we know that $B_m(0, k)$ is identically zero for all odd m. From (12) it follows that the odd cosine and sine coefficients of the perturbation q (as measured from the origin) cannot be recovered.

If we consider the finite dimensional situation, where there are $2N + 1$ basis trigonometric functions and M incident directions given by angles θ_0^i, $i = 1, \ldots; M$, then provided $M \geq 2N + 1$ the resulting system of equations is uniquely solvable for the coefficients $\{B_m(\gamma, k)\, \alpha_m\}_0^N$ and $\{B_m(\gamma, k)\, \beta_m\}_1^N$. The condition number of the resulting Gram matrix which has rows $[1, \cos m\theta_i, \sin m\theta_i]$, $1 \leq i \leq M$, $1 \leq m \leq N$, will depend on the choice of the directions of the incident waves. The condition number will be minimised by choosing an equal spread of the directions over $[0, 2\pi]$, whereas a concentration into a sector will result in very poor conditioning. As we will show in a later section the additional degree of ill-conditioning due to division by the term B_m is small.

This is summarised in

Theorem 1. *Let $0 < \gamma < 2\pi$. Then if the wavenumber k is sufficiently small the derivative map F'_{inc} is injective. In the finite dimensional problem with M incident waves from distinct directions and a finite trigonometric basis (7), the resulting Jacobian matrix has trivial nullspace provided $M \geq 2N + 1$.*

We now consider the multiple frequency, single incident direction problem. Here we assume that a single incident wave with direction angle θ_0 has the (complex) value of its far field pattern measured at a single angle $\theta = \theta_0 + \gamma$. The frequency of the wave is assumed to be vary over an interval $[k_{\min}, k_{\max}]$. We denote this map by F_{freq}. Due

to the rotational invariance of the circle, the derivative $F'_{\rm freq}(q)$ will depend only on the difference γ, so that without loss of generality, we may set $\theta_0 = 0$.

If we use the representation (12) and take into account the symmetry condition on $B_{-m} = (-1)^m B_m$ shown in Lemma 1, then we have

$$(F'_{\rm freq}q)(\gamma) = \sqrt{\frac{8}{\pi^2 k}}\, e^{i\frac{\pi}{4}} \left[\sum_{\substack{m=0 \\ m={\rm even}}}^{N} \alpha_m B_m(\gamma,k) + i \sum_{\substack{m=1 \\ m={\rm odd}}}^{N} \beta_m B_m(\gamma,k) \right]. \qquad (15)$$

It is immediately clear from this that one cannot recover the even numbered sine and the odd numbered cosine coefficients of the perturbation q defined by (8). On the other hand, if $F'_{\rm freq}(q) = 0$, then although nothing can be said about the coefficients $\alpha_{2\ell+1}$ and $\beta_{2\ell}$, it is clear that $B_{2\ell}(\gamma,k)\alpha_{2\ell} = 0$ and $B_{2\ell+1}(\gamma,k)\beta_{2\ell+1} = 0$. Now it is obvious that $B_m(\gamma,k)$ is analytic for $k > 0$ and hence we can use Lemma 2 to expand the derivative in terms of powers of k to obtain

$$(F'_{\rm freq}q)(\gamma) = \sqrt{8}\, e^{i\frac{\pi}{4}} \Big[\frac{\pi}{4}\alpha_0 \frac{1}{\ln^2 \frac{k}{2}} + (\pi i) \sin\frac{\gamma}{2}\, \beta_1 \frac{k}{\ln \frac{k}{2}} + \frac{\pi}{2} \cos\gamma\, \alpha_2 \frac{k^2}{\ln \frac{k}{2}} - \frac{\pi}{4}\alpha_2\, k^2 \, + \ldots \Big],$$

and equating terms in k we see that $F'_{\rm freq}(q)(\gamma) = 0$ implies that $\alpha_{2\ell} = 0$ and $\beta_{2\ell+1} = 0$, $\ell = 0, 1 \ldots$, provided that $0 < \gamma < 2\pi$. This is summarised in the following theorem:

Theorem 2. *For any γ with $0 < \gamma < 2\pi$, the nullspace of $F'_{\rm freq}$ consists of the odd numbered cosine and the even numbered sine coefficients (when expanded with the origin at $t = \frac{\gamma}{2}$).*

Is there complete loss of information if $\gamma = 0$? Certainly, as before, the odd cosine coefficients are still in the nullspace. In addition, we see from the above and Lemma 1 that all the sine coefficients are also in the nullspace. From Lemma 2 we see that $g_m(0) = 0$ for all m and $h_m(0) = 0$ for m odd. However, for m even, $h_m(0)$ is nonzero. Thus the nullspace of $F'_{\rm freq}$ when $\gamma = 0$ consists of all the sine coefficients and all the odd cosine coefficients.

Theorem 2 shows that the measurement of the far field at a single angle gives "one half" the amount of information required to reconstruct a sufficiently small perturbation of the circle. Thus for those perturbations q with a finite Fourier series with maximum frequency N the dimension of the nullspace of $F'_{\rm freq}$ is exactly N. The obvious question is, does measurements at a scan of frequencies at two distinct points recover full information? Since we have given a precise characterisation of the nullspace for a single measurement, we are able to answer this question in the affirmative:

Theorem 3. *From the values of the far field pattern measured at two angles γ_1 and γ_2 we can recover all Fourier coefficients in (7) provided $\gamma_1 \neq 0$ and $\gamma_2 \neq 0$ and*

$$\sin m\frac{(\gamma_1 - \gamma_2)}{2} \neq 0 \qquad \text{for } m = 1, \ldots, N. \qquad (16)$$

Proof: This follows directly from Theorem 2 and the fact that the pairs

$$\sin m\Big(t - \frac{\gamma_1}{2}\Big) \quad \text{and} \quad \sin m\Big(t - \frac{\gamma_2}{2}\Big)$$

and

$$\cos m\Big(t - \frac{\gamma_1}{2}\Big) \quad \text{and} \quad \cos m\Big(t - \frac{\gamma_2}{2}\Big)$$

are linearly independent if (16) is satisfied.

4. Some numerical methods for the reconstruction of the domain

Our approach to the numerical reconstruction will involve iterative methods to solve the nonlinear equation $F(\partial D) = u_\infty$. We seek a sequence of approximations $\{r_n\}$ to the obstacle boundary r generated by the scheme

$$r_{n+1} = r_n - \mathcal{A}_n(F(r_n) - u_\infty) \tag{17}$$

where the operator $\mathcal{A}$ uses derivative information from the map F, and u_∞ denotes the data obtained from measurements of the far field. That is, we seek to replace the operator equation (6) by its linearisation.

Two commonly used cases are $\mathcal{A}_n = \big(F'[r_n]\big)^{-1}$ (where $(F')^{-1}$ may mean the generalised inverse of F') or $\mathcal{A}_n = \big(F'[r_n]\big)^*$. The former leads to Newton-type schemes and the latter to Landweber-Fridman iteration. If the solution of (6) is to be considered as the least squares minimum of the objective functional $\|F(r) - u_\infty\|_2$, then taking $\mathcal{A} = \big(F'[r]^*F'[r]\big)^{-1}F'[r]^*$ gives a scheme that is usually referred to as the *Gauss-Newton method*. The choice $\mathcal{A}_n = \big(F'[r_n]\big)^*$ gives the *method of Steepest Descent.*

While the above considers the nonlinear nature of (6), we must also consider the ill-conditioning. In the Landweber scheme the usual implementation utilises a stopping criteria; when the residual, defined as the L^2 difference of the computed solution and actual data, no longer decreases then the scheme is terminated. The existence of such a stopping condition and the convergence of the iteration procedure requires the verification of certain conditions (see for example [HNS]) which we have not been able to show for the infinite dimensional operator $(F')^*$). For the finite dimensional problem these are trivially satisfied if we use the value of the derivative at a circle, since we have been able to show that F' is one to one (Theorems 1 and 3). However, this has not been proven for more general regions, nor can we guarantee that the rate of convergence will not slow down with increasing dimension of the underlying space.

In the Newton scheme we will also take a standard approach and seek a generalised inverse that is not only invertible, but has a sufficiently small condition number. One way to achieve this is by limiting the size of the basis set, that is, the value of N. Again, we have no guarantee that the Jacobian matrix will be invertible for non-circular regions, but in practice no difficulties were found. Since this limitation is equivalent to ignoring all frequencies in the boundary representation higher than N, this is simply just regularisation by spectral cut-off.

An alternative means to stabilise the inversion in the Newton scheme is to use Tichonov regularisation; replacing the inverse of F' by $\big(\alpha I + F'[r]^*F'[r]\big)^{-1}F'[r]^*$. We show a few reconstructions using this approach.

Of course we can combine the two methods to advantage by for example choosing $\mathcal{A}_n = \lambda_n I + \big(F'[r]^*F'[r]\big)^{-1}F'[r]^*$ for some sequence λ_n. This is the Levenberg-Marquardt idea and typically one uses a decreasing sequence $\{\lambda_n\}$ that has the effect weighting towards the more rapidly convergent Newton scheme once the initial approximation has been sufficiently improved to be within the often narrow domain of capture of this method. As we will point out later this may actually be an essential step.

For the solution of the forward problem generating the synthetic data u_∞ and evaluating F in each iteration step we used the Nyström method based on a combined double and single-layer boundary integral equation approach as presented in [CK]. In order to ensure the integrity of the procedure we used different coupling parameters in the combination of the double- and single-layer potentials. The synthetic data was

generated using only 16 grid points, so that the solution was only about 1% accurate. However, in the computation of the forward map F in the inverse problem solver a much finer grid was used; typically 60 or 80 points.

Our data consisted of a subset of the values of u_∞. In the case of multiple incident waves this is $u_\infty(d^j, \theta)$ where the M incident plane waves have incident directions d^j, $1 \le j \le M$, (corresponding to the angles of incidence θ_0^j) and the measurement point θ is determined by $\theta = \gamma + \theta_0^j$ for some fixed angle γ.

For the multiple frequency situation we have $M/2$ measurements of the scattered wave at both of the points $\theta_0 + \gamma_1$ and $\theta_0 + \gamma_2$, each at a different wavenumber k_j. Note that we are using both the real and imaginary parts of the far field, so that there are in fact $2M$ data values in each of the two inverse problems.

For a stopping rule for the scheme we used the relative residual

$$R_n := \Big(\sum_{j=1}^{M} |F(r_n) - u_\infty^j|^2\Big)^{\frac{1}{2}} \Big/ \Big(\sum_{j=1}^{M} |F(r_n)|^2\Big)^{\frac{1}{2}}$$

and terminated the procedure when the difference between the values of R_n for two consecutive iterations was less than a tolerance value δ. In our computations we used $\delta = 10^{-4}$. As a measure of accuracy for the reconstructions we used the L^2 error $\|r_n - r_{\rm act}\|_2$.

The corresponding reconstructions are illustrated in Figures 1 and 2. The dashed lines give the exact boundary curves and the full lines give the reconstructions. The starting approximation r_0 in each case was the unit circle and this is also shown on each figure. The number of iterations required for each reconstruction is indicated along with the final L^2 norm of the difference of the reconstructed and actual boundaries.

For the case of multiple incident plane waves Figure 1 shows reconstructions of three obstacles; an ellipse, a bean-shape and a figure with three lobes,

$$r(t) = \frac{1}{1 + C\cos t}, \qquad \frac{1 + 0.9\cos t + 0.1\sin 2t}{1 + 0.75\cos t}, \qquad 0.5 + 0.25e^{-\sin 3t} - 0.1\sin t$$

In these numerical experiments we chose 16 equally spaced directions. The (fixed) wavenumber was $k = 1$. Various values of the offset angle γ was used. Theoretically, the backscattered case ($\gamma = \pi$) should give optimal results, but in fact we found very little difference in the quality of the reconstructions provided γ was chosen greater than about $\pi/10$. In the case of forward scattering ($\gamma = 0$), we even were able to obtain an excellent reconstruction of a curve whose Fourier coefficients were relatively small in the direction of the nullspace of $F'[r = 1]$ by using a singular value decomposition of the Jacobian and simply ignoring all directions in the nullspace of F'. The number of iterations required for numerical convergence varied very little with the shape of the object; on average, about 10 iterations were necessary to satisfy the stopping criterion. Since the data was obtained through a course mesh size in the direct scattering numerical scheme these figures should be considered as being obtained under about 1% error, which in this case is liable to be systematic rather than random.

Reconstructions of the same three test obstacles using data consisting of a set of incident plane waves with common direction but with a range of frequencies is shown in Figure 2. We have used arrows to represent the incident direction d, while the marks $\triangle$ indicate the two locations where the far field pattern was measured. In each case

Fig 1. Reconstruction using spectral-cut-off from 16 incident waves .

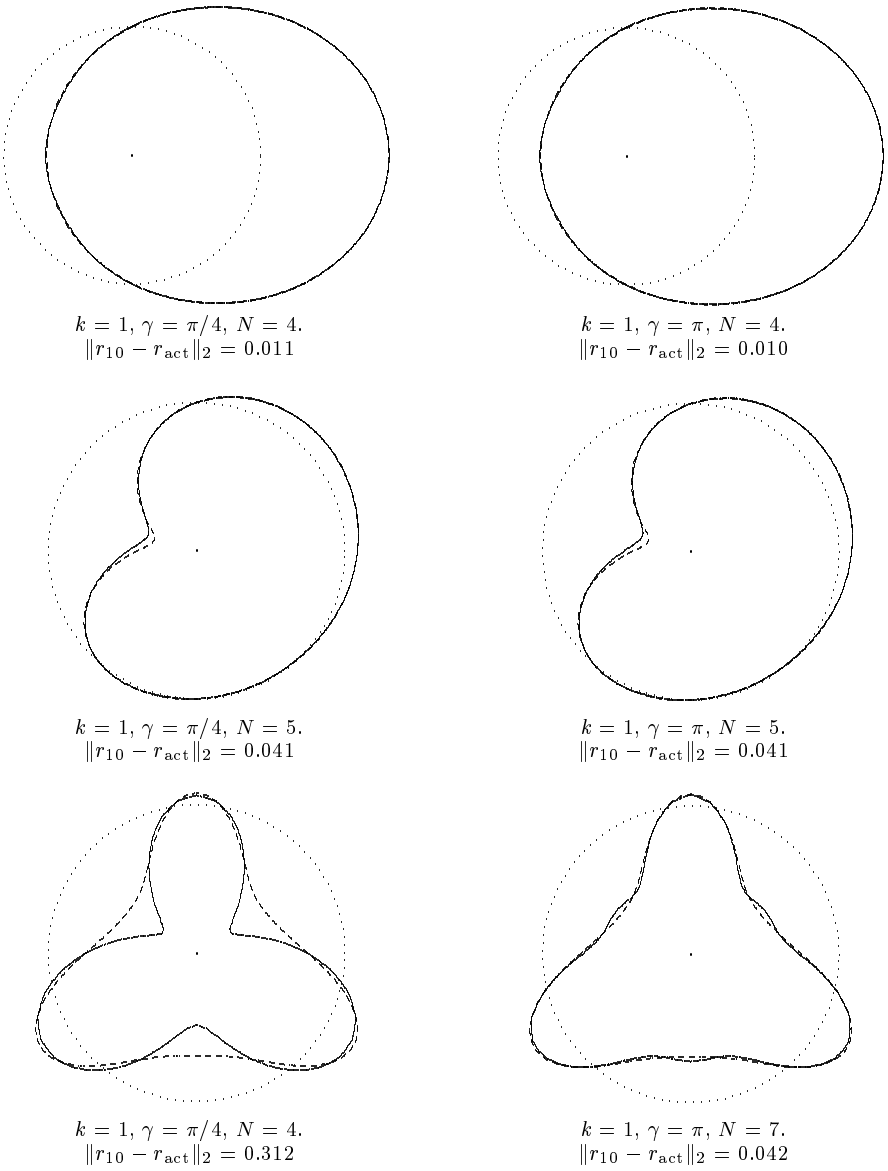

$k = 1, \gamma = \pi/4, N = 4.$
$\|r_{10} - r_{\text{act}}\|_2 = 0.011$

$k = 1, \gamma = \pi, N = 4.$
$\|r_{10} - r_{\text{act}}\|_2 = 0.010$

$k = 1, \gamma = \pi/4, N = 5.$
$\|r_{10} - r_{\text{act}}\|_2 = 0.041$

$k = 1, \gamma = \pi, N = 5.$
$\|r_{10} - r_{\text{act}}\|_2 = 0.041$

$k = 1, \gamma = \pi/4, N = 4.$
$\|r_{10} - r_{\text{act}}\|_2 = 0.312$

$k = 1, \gamma = \pi, N = 7.$
$\|r_{10} - r_{\text{act}}\|_2 = 0.042$

the difference in the angles γ_1 and γ_2 was chosen so that the condition in Theorem 3 was satisfied for the values of N used. Note that this condition is known to hold only when the obstacle is the unit circle. We used 20 frequencies chosen randomly from the interval $[0.5, 2.0]$. As the numerical scheme progressed we monitored the values of the condition number κ of the Jacobian matrix, but actually found little difference from the sort of values obtained when the scatterer was a circle. (A typical range was $\kappa = 5$ for $N = 2$ to about $\kappa = 500$ for $N = 6$ with careful choice of $\gamma_1 - \gamma_2$.)

As in the previous problem, ten iterations was usually sufficient to reconstruct a wide variety of obstacles. However, for regions not close to the initial approximation, the Newton scheme would often not converge, but in fact would rapidly diverge within a

few iterations. If we first take a small number (typically, 5 was used) of Landweber steps to improve the starting approximation, then the Newton scheme was often able to take over resulting in rapid convergence. This was the case for the three-lobed region. Of course, a more sophisticated Levenberg-Marquardt scheme could be developed where the choice of the parameter λ_n could be made on the basis of the current values of the residuals, rather than taking λ_n very large for $n \leq 5$ and then $\lambda_n = 0$ for $n > 5$.

Fig 2. Reconstruction using 20 wavenumbers at two measurement points

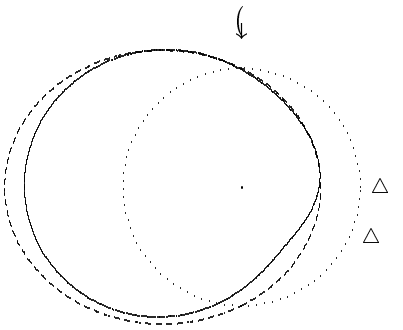

Frozen Newton, spectral cut-off, $N = 3$.
$\theta_0 = \pi/2$, $\gamma_1 = 0.5\pi$, $\gamma_2 = 0.68\pi$.
$\|r_{30} - r_{\text{act}}\|_2 = 0.231$

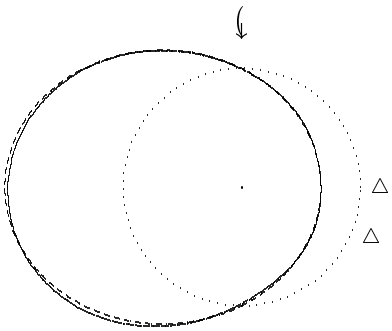

Full Newton, spectral cut-off, $N = 5$.
$\theta_0 = \pi/2$, $\gamma_1 = 0.5\pi$, $\gamma_2 = 0.68\pi$.
$\|r_7 - r_{\text{act}}\|_2 = 0.036$

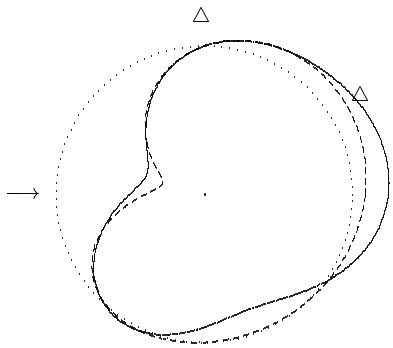

Full Newton, spectral cut-off, $N = 3$.
$\theta_0 = 0$, $\gamma_1 = 0.5\pi$, $\gamma_2 = 0.73\pi$.
$\|r_{10} - r_{\text{act}}\|_2 = 0.203$

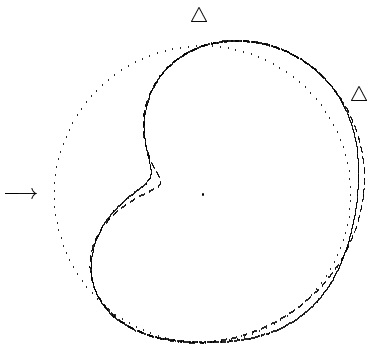

Full Newton, spectral cut-off, $N = 5$.
$\theta_0 = 0$, $\gamma_1 = 0.5\pi$, $\gamma_2 = 0.73\pi$.
$\|r_{10} - r_{\text{act}}\|_2 = 0.078$

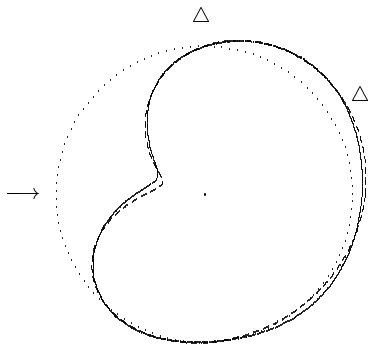

Landweber-Newton, Tichonov, $\alpha = 0.02$.
$\theta_0 = 0$, $\gamma_1 = 0.5\pi$, $\gamma_2 = 0.73\pi$.
$\|r_{13} - r_{\text{act}}\|_2 = 0.076$

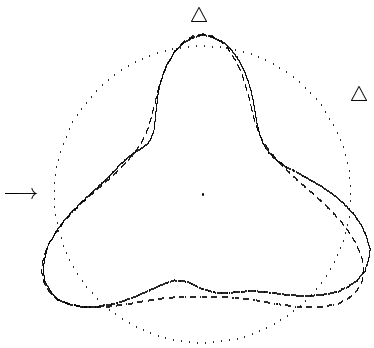

Landweber-Newton, Tichonov, $\alpha = 0.02$.
$\theta_0 = 0$, $\gamma_1 = 0.5\pi$, $\gamma_2 = 0.73\pi$.
$\|r_{12} - r_{\text{act}}\|_2 = 0.147$

We also attempted to reconstruct objects using a frozen Newton scheme – where the derivative is held fixed at the initial approximation, in our case the unit circle. Thus in (17) we take $\mathcal{A}_n \equiv \mathcal{A}_0$. This approach has two advantages. First, we are able to prove that the matrix we are using is actually invertible. Second, the additional cost of computing the derivative $F'(r_n)$ is avoided. Computing this requires the solution of a second scattering problem (see [KR1]) which increases the computational cost of each iteration by approximately a factor of two. The disadvantage, of course, is that the value of the derivative may vary considerably even in a neighbourhood of the origin and the resulting method will lose some of the power of the full Newton scheme, or, even fail to converge at all.

In the case of recovering an obstacle from a single plane wave, but where the far field pattern was measured in all directions, [KR1], this frozen Newton scheme gave results that were for the most part indistinguishable from when the actual derivative was used at each step.

However, for the case of multiple frequency data the situation was quite different; we were only able to recover obstacles that were close to a circle. In Figure 2 an example is shown of the frozen Newton being used to reconstruct the ellipse. Note the poorer reconstruction than that obtained by updating the derivative at each stage. There was an additional cost since the frozen Newton scheme required four times as many iterations to achieve these results; thus the total computational cost was approximately twice as much. We were able to reconstruct an ellipse with eccentricity less than 1.5 about equally well with both the full and frozen Newton schemes, although with many more iterations being required in the latter case. If the eccentricity was greater than 2 then the frozen Newton scheme failed. If it were increased to about 2.5 then even the full Newton scheme would fail unless a better initial approximation was obtained by using several Landweber steps.

It was also noted that our schemes would sometimes obtain obstacles different from the actual figure and these reconstructions would depend on the parameters such as size of basis and initial approximation. This is usually an indication of the existence of additional local minima in the associated optimisation problem.

In some sense these results bear out other evidence gleaned from numerical experiments and some analysis. The scattering problem consisting of a single incident wave at a fixed frequency with measurements on all of Ω is highly ill-posed; the effective Jacobian of the boundary to data map increases exponentially in N [KR1]. The incident wave at multiple frequency problem appears to lead to a derivative with a smaller condition number with a consequent decrease in ill-posedness. However, the later problem appears to be "more nonlinear" than the former.

5. References

[CK] Colton, D., and Kress, R: *Inverse Acoustic and Electromagnetic Scattering Theory.* Springer-Verlag, Berlin Heidelberg New York 1992.

[CS] Colton, D., and Sleeman, B.D: Uniqueness theorems for the inverse problem of acoustic scattering. IMA J. Appl. Math. **31**, 253–259 (1983).

[ER1] Eskin, G., and Ralston, J: Inverse backscattering in two dimensions, Comm. Math. Phys. **138**, (1991), no. 3, 451–486.

[ER2] Eskin, G., and Ralston, J: The inverse backscattering problem in three dimensions, Comm. Math. Phys. **124**, (1989), no. 2, 169–215.

[HNS] Hanke, M., Neubauer, A. and Scherzer, O.: A convergence analysis for the Landweber iteration for nonlinear ill-posed problems. Numer. Math. **72**, 21–37 (1995).

[Ki] Kirsch, A: The domain derivative and two applications in inverse scattering theory. Inverse Problems **9**, 81–96 (1993).

[KR1] Kress, R., and Rundell, W: A quasi-Newton method in inverse obstacle scattering, Inverse Problems **10**, 1145–1157 (1994).

[KR2] Kress, R., and Rundell, W: Inverse obstacle scattering with modulus of the far field pattern as data. In: *Inverse Problems in Medical Imaging and Nondestructive Testing,* (Engl, Louis, Rundell eds.) Springer-Verlag, Wien, New York 1997.

[LN] Liu, C., and Nachman, A: A scattering theorem analog of a theorem of Pólya and an inverse obstacle problem, to appear.

[LP] Lax, P.D., and Phillips, R.S: *Scattering Theory.* Academic Press, New York 1967.

[Po] Potthast, R: On a concept of uniqueness in inverse scattering for a finite number of incident waves." SIAM J. Appl. Math., to appear.

[SU] Stefanov, P. and Uhlmann, G: Inverse backscattering for the acoustic equation. SIAM J. Math. Anal., to appear.